Schottky barrier junctions of hydrogenated amorphous silicon-germanium alloys

Hideharu Matsuura and Hideyo Okushi
Electrotechnical Laboratory, 1-1-4 Umezono, Sakura-mura, Niihari-gun, Ibaraki 305, Japan

(Received 10 February 1987; accepted for publication 9 June 1987)

The current-transport mechanisms of amorphous Schottky barrier junctions are investigated using both undoped and phosphorus-doped hydrogenated amorphous silicon-germanium alloys (a-$Si_{1-x}Ge_x$:H) fabricated by rf glow discharges in diode- and triode-reactor systems with and without the dilution of hydrogens. From the experimental results, the forward-current mechanisms for amorphous Schottky barrier junctions are generally discussed and classified into three categories: (1) field emission, (2) diffusion-field emission, and (3) diffusion. The diffusion-field-emission model (multistep tunneling through a part of the Schottky barrier) used for the first time in this work can interpret the current-voltage characteristics and their temperature dependence on amorphous Schottky barrier junctions to a high degree. Moreover, the flow chart proposed here classifies the material quality of amorphous semiconductors according to their junction properties. We concluded that one of the better methods to fabricate high-quality a-$Si_{1-x}Ge_x$:H for Schottky barrier junctions is the triode-reactor technique using hydrogen-diluted starting-gas materials.

I. INTRODUCTION

Since the first substitutional doping of hydrogenated amorphous silicon (a-Si:H) was achieved by the glow-discharge decomposition of SiH_4 mixed with either PH_3 or B_2H_6,[1] a-Si:H has been a highly important material for devices such as solar cells[2] and thin-film transistors.[3] Recently, a hydrogenated amorphous silicon-germanium alloy (a-$Si_{1-x}Ge_x$:H) has been applied to enhance the performance of amorphous solar cells.[2] However, there have been few reports on the junction transports of amorphous materials[4] except for a-Si:H.[5–16] Since the film quality of a-$Si_{1-x}Ge_x$:H (Refs. 17 and 18) and a-Si:H can be changed greatly, the general aspects of the junction transports peculiar to amorphous semiconductors can be discussed using the junction properties of a-$Si_{1-x}Ge_x$:H and a-Si:H.

Schottky barrier junctions are fabricated using a simple metal-deposition technique, and are employed as useful and important tools for investigating the nature of semiconductor materials and the properties of junctions. Although the transport mechanisms of Schottky barrier junctions for crystalline semiconductors have been completely elucidated,[19] those for amorphous semiconductors have not yet been established. Therefore, they have been discussed on the basis of crystalline-semiconductor theories for the diffusion and recombination mechanisms within the depletion region.[20] Because of the many defects in amorphous films, Schottky barrier junctions of amorphous semiconductors differ from those of crystalline counterparts in that: (1) carrier collisions in the depletion region cannot be ignored; (2) the effect of surface states in amorphous semiconductors is probably much smaller than in crystalline counterparts; and (3) multistep tunneling through the Schottky barrier occurs easily.[12]

In this paper, we fabricated Schottky barrier junctions using several a-$Si_{1-x}Ge_x$:H films as well as a-Si:H films, and investigated the change of the junction-transport mechanisms from low-grade films to high-grade ones. It has not yet been determined experimentally whether Schottky barrier diodes on a-Si:H exhibit predominantly thermionic emission[7,9,11,14] or diffusion characteristics.[6,8,15] Because of the higher density of gap states in a-$Si_{1-x}Ge_x$:H than in a-Si:H, we will assume that the limiting mechanism of transport through the depletion region and into the metal will be the diffusion of electrons throughout our analysis. The general aspects of amorphous Schottky barrier junctions are discussed using the results gained. We also propose a flow chart to classify amorphous semiconductors into six grades from the viewpoint of their junction properties.

II. EXPERIMENT

Undoped and phosphorus (P)-doped a-$Si_{1-x}Ge_x$:H films were deposited by the glow-discharge decomposition of GeH_4/SiH_4 and $GeH_4/SiH_4/PH_3$ gas mixtures, respectively, under three different modifications: group X, using a conventional diode-type reactor [see Fig. 1(a)]; group Y, using a triode-type reactor with a mesh electrode between the anode and the cathode [see Fig. 1(b)]; and group Z, using a triode-type reactor and a H_2-diluted gas mixture.

Corning 7059 glass and n^+ crystalline Si (c-Si) were used as substrates for measuring conductivity of films and current-voltage characteristics of diodes, respectively. The

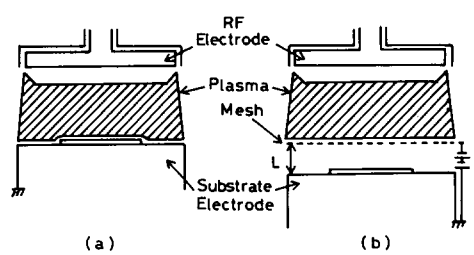

FIG. 1. Schematic sketches of two glow-discharge reactor systems: (a) diode and (b) triode. The hatched area indicates the glow-discharge plasma space.

 0021-8979/87/192871-09$02.40

TABLE I. Deposition conditions. Substrate temperature: 250 °C. rf frequency: 13.56 MHz.

Group	Type of chamber	rf power (W)	Pressure (mTorr)	Applied voltage of mesh electrode (V)
X	diode	40	25	
Y	triode	40	25	−200
Z	triode (H_2 dilution)	10	100	−150

deposition conditions are summarized in Table I and the doping-gas ratios are shown in Table II. Optical gap E_0 determined by the Tauc plots of $\sqrt{\alpha h\nu} = B(h\nu - E_0)$ is maintained at 1.5 eV for all samples while the other conditions and the film properties were as previously reported.[17,18]

The dark conductivities and photoconductivities were measured using coplanar electrode geometry. The metal-semiconductor junctions were fabricated by depositing the a-$Si_{1-x}Ge_x$:H films onto n^+ c-Si and then evaporating gold (Au) and magnesium (Mg) onto the a-$Si_{1-x}Ge_x$:H films. The current density with respect to voltage characteristic (J-V) was measured in a vacuum as a function of temperature over the range between 151 and 295 K, and for the undoped film it was measured between 295 and 350 K. Hysteresis was not an observed characteristic when the diodes were cooled and heated cyclically. The capacitance-voltage (C-V) characteristics of these diodes were measured over the frequency range between 1 Hz and 10 kHz at room temperature.

III. RESULTS

A. Doping-level dependencies of dark conductivities and photoconductivities

Figure 2 shows the doping-level dependencies of the dark conductivities and photoconductivities (σ_d,$\Delta\sigma_p$) of a-$Si_{1-x}Ge_x$:H films for the three groups. The numbers for each group correspond to the doping-gas ratios and are fully described in Table II. As shown in Fig. 2, the ratio of $\Delta\sigma_p$ to σ_d becomes higher in the order of $X1$, $Y1$, $Z1$ while $\Delta\sigma_p$ becomes higher in the order of X, Y, Z for each similar doping-gas ratio, suggesting that the a-$Si_{1-x}Ge_x$:H films in group Z have the lowest localized state density of the three groups. Indeed, the Ge ($g = 2.017$) dangling bond density determined by electron-spin-resonance (ESR) measurements[17] were found to be 5×10^{17}, 4×10^{16}, and 2×10^{16} cm^{-3} in undoped a-$Si_{1-x}Ge_x$:H for $X1$, $Y1$, and $Z1$, respectively.

TABLE II. Doping-gas ratio [PH_3/(SiH_4 + GeH_4 + PH_3)] (ppm).

Group X	Group Y	Group Z
$X1$: 0	$Y1$: 0	$Z1$: 0
$X2$: 67.3	$Y2$: 0.084	$Z2$: 7.75
$X3$: 905	$Y3$: 67.3	$Z3$: 76.3
$X4$: 7900	$Y4$: 905	$Z4$: 1080
	$Y5$: 7900	

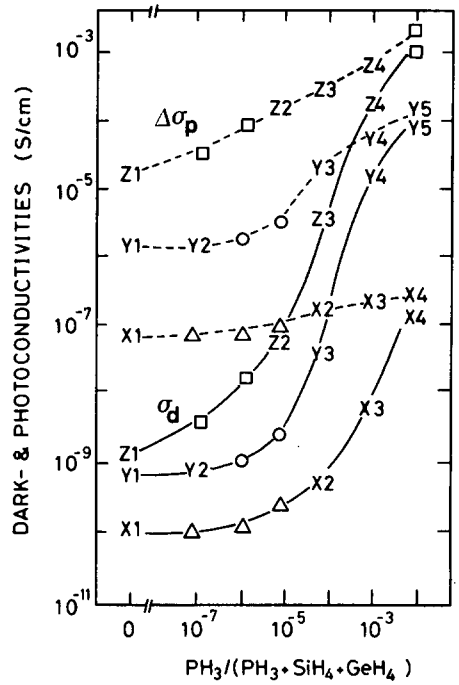

FIG. 2. Doping-level dependence of dark conductivities and photoconductivities (σ_d,$\Delta\sigma_p$) for three groups.

B. Contact property

The J-V characteristics of the Mg/a-$Si_{1-x}Ge_x$:H/n^+ c-Si and the Au/a-$Si_{1-x}Ge_x$:H/n^+ c-Si diodes were measured in order to investigate the contact properties of

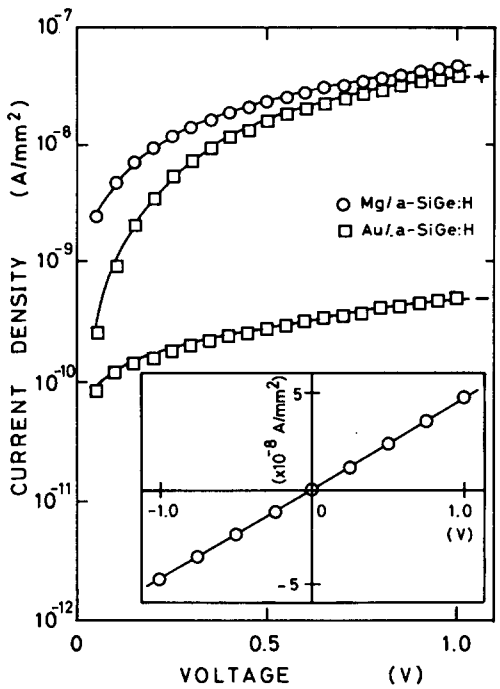

FIG. 3. J-V characteristics of Mg/a-$Si_{1-x}Ge_x$:H/n^+ c-Si and Au/a-$Si_{1-x}Ge_x$:H/n^+ c-Si diodes with film $Y1$ and also linear-scaled J-V curve of the diode using Mg is inserted. Symbols + and − represent data for positive- and negative-bias voltages on the metal, respectively.

a-$Si_{1-x}Ge_x$:H/n^+ c-Si. For example, those of Y 1 are shown in Fig. 3 with the symbols + and − representing data for positive- and negative-bias voltages on the metal, respectively. The diode using Mg shows an ohmic property, but that using Au exhibits a rectifying property, as shown by the figure. This result indicates that the contact of n^+ c-Si/a-$Si_{1-x}Ge_x$:H as well as that of Mg/a-$Si_{1-x}Ge_x$:H is ohmic. The contact of Au/a-$Si_{1-x}Ge_x$:H therefore forms the Schottky barrier junction. The contact properties of the other films are similar to those of Y 1. These properties are similar to undoped and P-doped a-Si:H (Refs. 10 and 13) and all the films are n-type semiconductors. In the following results, data of the structure of Au/a-$Si_{1-x}Ge_x$:H/n^+ c-Si are only included to describe the Au/a-$Si_{1-x}Ge_x$:H Schottky barrier junctions.

C. Current-voltage characteristics

Figure 4 shows the J-V characteristics of the Au/a-$Si_{1-x}Ge_x$:H Schottky barrier junctions for various doping-gas ratios, $PH_3/(PH_3 + SiH_4 + GeH_4)$, for group X. Poor rectifying properties were exhibited because of the high density of localized states. Two possible reasons explaining this fact are (i) the tunneling process through the thin Schottky barrier and (ii) the recombination process within the depletion region.

The doping-level dependencies of the J-V characteristics for groups Y and Z are shown in Figs. 5 and 6, respectively. The Au/a-$Si_{1-x}Ge_x$:H junctions of groups Y and Z exhibit good rectifying properties when compared with group X. Although the dark conductivities of Z 1, Z 2, and Z 4 are close to Y 2, Y 3, and Y 5 as shown in Fig. 2, respectively, the rectifying ratios of the Au/a-$Si_{1-x}Ge_x$:H Schottky barrier junctions for group Z are better than those of the corresponding junctions for group Y. The sample Z 1 of undoped

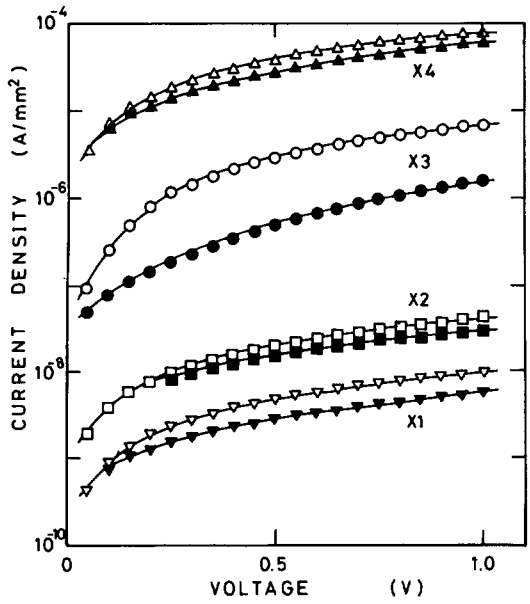

FIG. 4. Doping-level dependence of J-V characteristics of Au/a-$Si_{1-x}Ge_x$:H junctions in group X. Open and solid marks represent data points for positive- and negative-bias voltages on the metal, respectively.

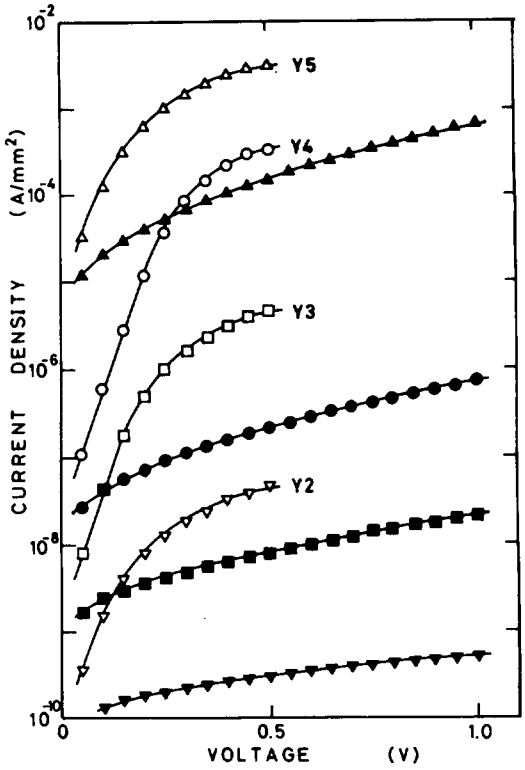

FIG. 5. Doping-level dependence of J-V characteristics of Au/a-$Si_{1-x}Ge_x$:H junctions in group Y. Open and solid marks represent data points for positive- and negative-bias voltages on the metal, respectively.

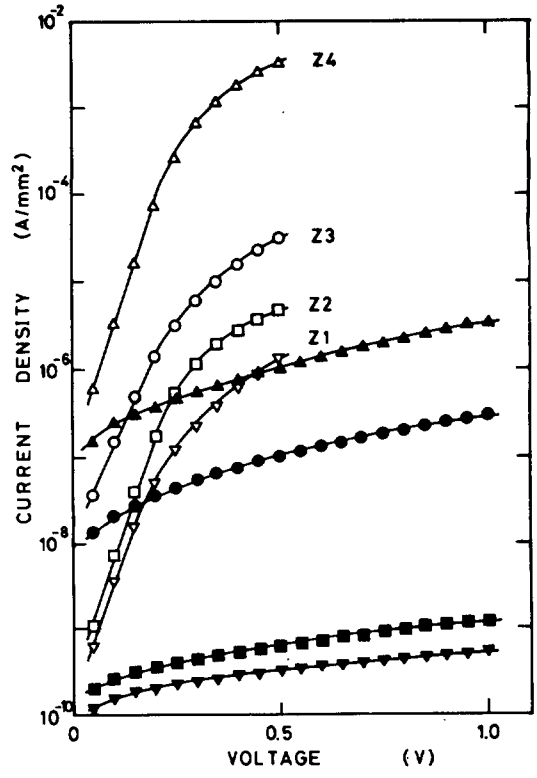

FIG. 6. Doping-level dependence of J-V characteristics of Au/a-$Si_{1-x}Ge_x$:H junctions in group Z. Open and solid marks represent data points for positive- and negative-bias voltages on the metal, respectively.

a-$Si_{1-x}Ge_x$:H in Fig. 6 exhibits a worse rectifying property than that of a-Si:H with the similar conductivity ($\sim 10^{-9}$ S/cm), that is, the reverse current ($\sim 10^{-10}$ A/mm^2) of the a-$Si_{1-x}Ge_x$:H sample $Z1$ is larger than that ($\sim 10^{-13}$ A/mm^2) of the a-Si:H diode.[15]

D. Temperature dependence of J-V characteristics

The temperature dependencies of the J-V characteristics were measured in order to investigate the current-transport mechanism for these Schottky barrier junctions in detail. From the linear region on a semilog scale of the J-V characteristics at various temperatures, the temperature dependencies of the slope β and the η value were estimated graphically using the following equations:

$$J = J_{0T} \exp(\beta V) \tag{1}$$

and

$$J = J_{0D} \exp(qV/\eta kT), \tag{2}$$

where J_{0T} and J_{0D} are the saturated current densities.

Although the linear regions could not be obtained in group X, they could be obtained in the case of groups Y and Z. Figure 7 shows the results for sample $Z4$, for different temperatures. Therefore, Eqs. (1) and (2) could be available to most of the samples in groups Y and Z; the temperature dependencies of β and the η value of typical samples ($Y4$, $Z2$, $Z4$) are shown in Figs. 8 and 9, respectively. The slope β for sample $Y4$ is almost independent of the measuring temperature as shown in Fig. 8, indicating that the tunneling current (the field-emission current[21]) is assumed to be predominant in sample $Y4$. This result seems very reasonable because the barrier width becomes thin due to heavy P doping. The fact that the η values of sample $Z2$ are close to 1.1 in Fig. 9 proves that the recombination current is not dominant.[20]

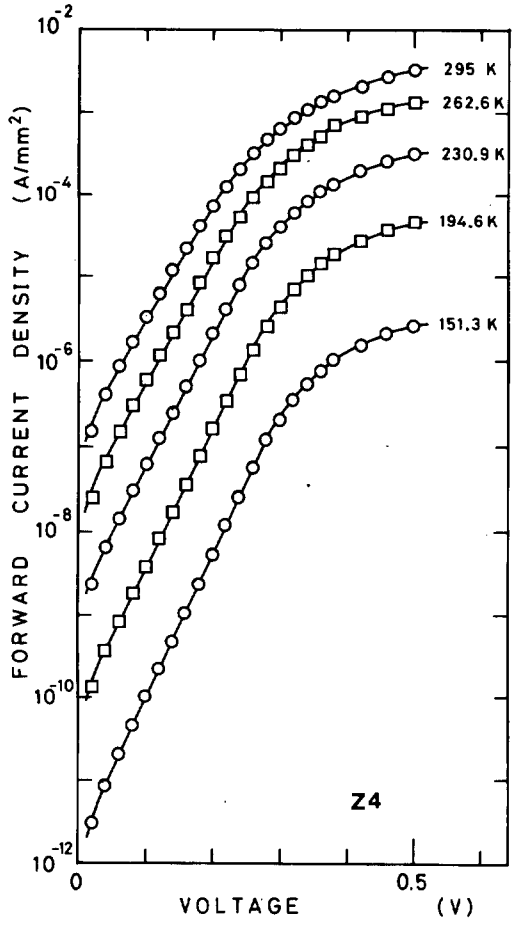

FIG. 7. Temperature dependence of forward currents of sample $Z4$. Linear regions on a semilog scale is clearly obtained in the whole range of the temperatures.

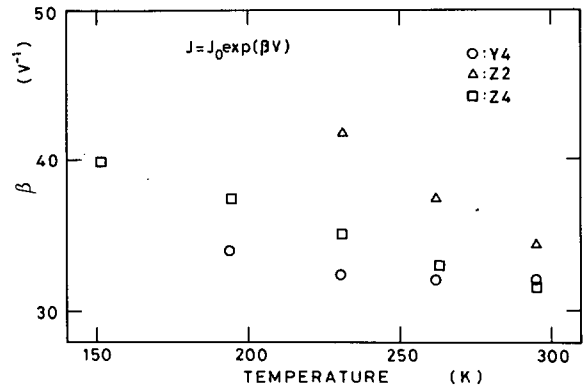

FIG. 8. Temperature dependence of slope β.

The activitation energies ΔE_1 and ΔE_2 of the forward currents having bias values of 0.05 and 1 V, respectively, can be obtained from the slope of the Arrhenius' plots (J-$1/T$). Those data are shown in Table III. The activation energy ΔE_1 represents that of the forward current which increases exponentially with the applied voltage, indicating that ΔE_1 is related to the junction transport of Au/a-$Si_{1-x}Ge_x$:H. Because the forward current biased at 1 V is limited by the resistance of the a-$Si_{1-x}Ge_x$:H bulk, the value of ΔE_2 represents the energy difference between the bottom of the conduction band and the Fermi level.

E. Capacitance-voltage characteristics

The capacitance-voltage characteristics were measured at the adequate frequency which depends on the resistivity of the a-$Si_{1-x}Ge_x$:H bulk. As a typical result, the $1/C^2$-V characteristics of sample $Z4$ measured at 10 kHz are shown in

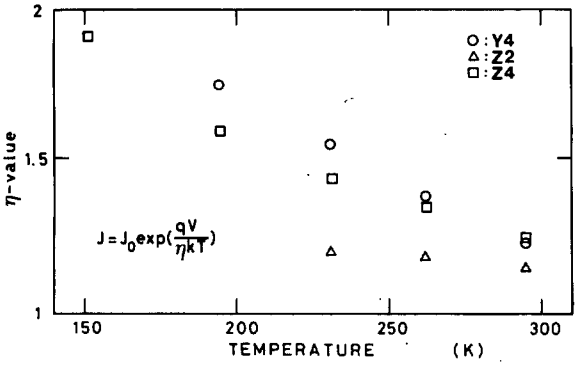

FIG. 9. Temperature dependence of the η value.

TABLE III. Experimental results obtained from J-V and C-V characteristics. ΔE_1: Activation energy of forward current biased at 0.05 V. ΔE_2: Activation energy of forward current biased at 1 V.

	J-V		C-V		
Sample number	ΔE_1 (eV)	ΔE_2 (eV)	N_I ($\times 10^{16}$ cm^{-3})	qV_D (eV)	Measuring frequency (Hz)
$Y3$	0.574	0.443	5.84	0.508	10^2
$Y4$	0.371	0.268	14.4	0.519	10^3
$Z1$	0.844	0.587	...	...	...
$Z2$	0.592	0.406	2.39	0.588	10^2
$Z4$	0.375	0.206	15.4	0.459	10^4
a-Si:H	1.03	0.721	0.52	0.446	10^{-2}[a]

[a] Low-frequency triangle-wave method (Ref. 22).

Fig. 10. The effective density N_I of the localized states can be graphically obtained from the slope of the figure, such as 1.54×10^{17} cm^{-3} for sample $Z4$. This is an important parameter because it determines the shape and width of the Schottky barrier. From the intercept on the voltage axis in Fig. 10, the built-in potential qV_B could be determined as 0.459 eV. The values of other samples are shown in Table III.

F. Estimation of barrier height

The quantity $q\phi$ is given by the sum of the activation energy ΔE_1 and the forward-bias potential qV as follows:

$$q\phi = \Delta E_1 + qV. \tag{3}$$

According to the diffusion theory,[19] $q\phi$ should approach the barrier height $q\phi_B$ if the current is limited by the diffusion. The value of $q\phi$ (0.894 eV) of a-$Si_{1-x}Ge_x$:H sample $Z1$ is lower than $q\phi$ (1.08 eV) of the a-Si:H sample having a reverse current of about 10^{-13} A/mm^2. This result is consistent with the fact that the level of the reverse current of sample $Z1$ is larger than that of the a-Si:H sample.

The barrier height ($q\phi_B$) can be estimated as the sum of the built-in potential (qV_B) and the Fermi level in the bulk ($\sim\Delta E_2$), as follows:

$$q\phi_B \simeq qV_B + \Delta E_2. \tag{4}$$

In the case of our Au/a-Si:H junction, $q\phi$ (1.08 eV) is close to $q\phi_B$ (1.17 eV) (Ref. 22) and the η value (<1.1) (Ref. 23) does not depend on the temperature, indicating that this current is limited by the diffusion in the depletion region.

In the case of sample $Z2$, however, $q\phi$ (0.642 eV) is much lower than $q\phi_B$ (0.994 eV), although the η value is close to 1.1 for the entire temperature range. This result suggests that the current is not limited by the diffusion but is mainly maintained by the tunneling at an upper part of the Schottky barrier in sample $Z2$.

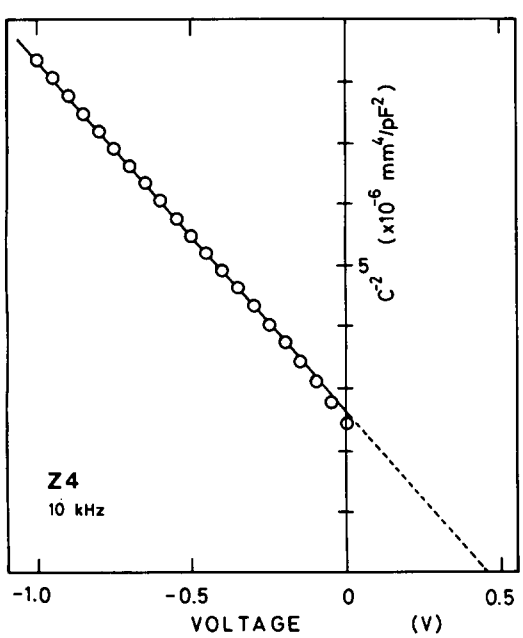

FIG. 10. Capacitance-voltage characteristics of sample $Z4$. Good linear relation between $1/C^2$ and V is obtained.

IV. DISCUSSION

A. Theoretical analysis

According to the thermionic-emission theory[19] for crystalline semiconductors, the shape of the barrier profile is immaterial and the current flow depends solely on the barrier height since it is assumed that electron collisions within the depletion region can be neglected. The various ways in which electrons can be transported across the Schottky barrier junction under forward bias are shown schematically for an n-type crystalline semiconductor in Fig. 11(a). The mechanisms are as follows:

(a) the emission of electrons from the semiconductor over the top of the barrier into the metal (the thermionic-emission current J_T);

(b) quantum-mechanical tunneling through a part of the barrier (the thermionic-field-emission current J_{TF});

(c) quantum-mechanical tunneling through the barrier from the edge of the depletion region (the field-emission current J_F); and

(d) recombination in the depletion region (the recombination current J_R).

It is possible to make practical Schottky barrier diodes in which (a) is the most important; these diodes are generally referred to as being nearly ideal. Processes (b), (c), and (d) cause departures from this ideal behavior while processes (b) and (c) appear only in the case of degenerated semiconductors at low temperature.[21,24–28]

In amorphous semiconductors, on the other hand, electron collisions within the depletion region cannot be neglected because of the existence of many defects. This means that the diffusion current J_D of Fig. 11(b) is more important to amorphous Schottky barrier junctions than J_T [Fig. 11(a)].

In actual amorphous Schottky barrier junctions, besides the diffusion current (J_D), the recombination current (J_R), and the tunneling currents (J_{DF} and J_F) due to multistep tunneling via localized states in the depletion region flow across the Schottky barrier as shown in Fig. 11(b).

In the case of nondegenerated crystalline semiconductors, J_{DF} in Fig. 11(b) is not taken into account in the current transport because tunneling via localized states in the depletion region can be neglected. J_{DF} is one of the concepts

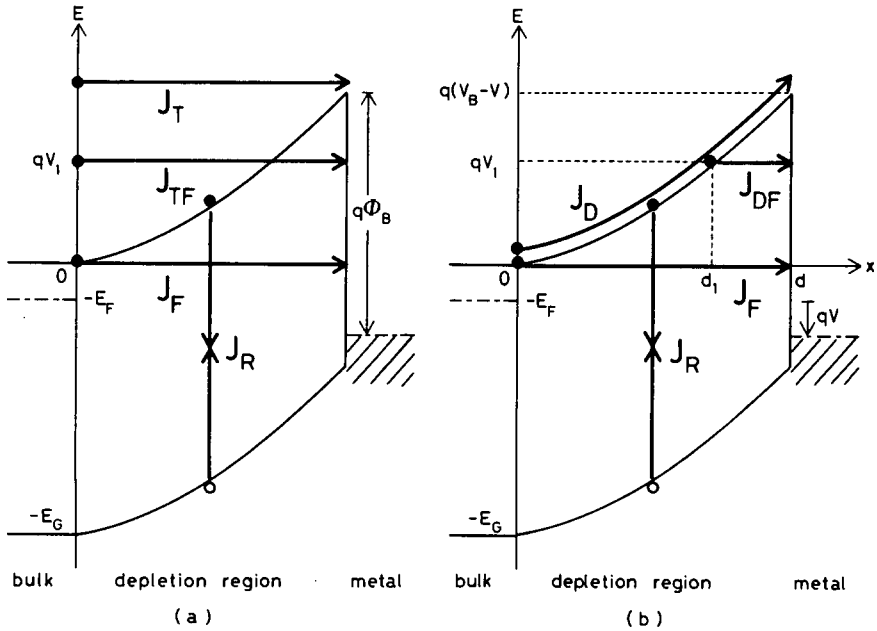

FIG. 11. Band diagrams for Schottky barrier semiconductor junctions with definitions of symbols defined in the text. The various current paths, (a) in crystalline and (b) in amorphous semiconductors, are also indicated.

peculiar to amorphous junctions (here, J_{DF} is the diffusion-field-emission current).

A theoretical approach to J_{DF} requires that the theories for crystalline Schottky barrier junctions be reviewed in order to discuss the junction transports peculiar to amorphous counterparts. The thermionic-emission current[19] from the semiconductor to the metal can be described as

$$J_T = \int_{q(V_B - V)}^{\infty} q v_x(E) N(E) f(E) dE, \tag{5}$$

where $v_x(E)$ is the velocity of electrons toward the metal, $f(E)$ the Fermi function, and where $N(E)$ is the density of states above the bottom of the conduction band at the edge ($x = 0$) of the depletion region and given by

$$N(E) = [4\pi(2m^*)^{3/2}/h^3]E^{1/2}, \tag{6}$$

with m^* being the effective mass of electrons and h Planck's constant. It is postulated that the kinetic energy of electrons in the conduction band can be expressed as

$$E = \tfrac{1}{2}m^* v^2, \tag{7}$$

where v is the electron velocity. Therefore, the thermionic-emission current is derived as

$$J_T = A^* T^2 \exp(-q\phi_B/kT)\exp(qV/kT), \tag{8}$$

with

$$A^* = 4\pi q m^* k^2/h^3. \tag{9}$$

The tunneling probability[26] at the energy of qV_1 can be given as

$$P \propto \exp\left(-\frac{4\pi}{h}(2m^*)^{1/2}\int_{d_1}^{d}(E - qV_1)^{1/2}\,dx\right), \tag{10}$$

with

$$E = (q^2 N_I/2\epsilon_s\epsilon_0)x^2 \tag{11}$$

and

$$qV_1 = (q^2 N_I/2\epsilon_s\epsilon_0)d_1^2, \tag{12}$$

where ϵ_0 is the free-space permittivity, ϵ_s the dielectric constant, d the width of the depletion region, and N_I the effective density of the localized gap states obtained from the slope of $1/C^2$-V characteristics. Substitution of Eqs. (11) and (12) into Eq. (10) gives

$$P \propto \exp\left(-\frac{qN_I}{\epsilon_0\epsilon_s E_{00}}\int_{d_1}^{d}(x^2 - d_1^2)^{1/2}\,dx\right) \tag{13}$$

with

$$E_{00} = (h/4\pi)\sqrt{(N_I/m^*\epsilon_0\epsilon_s)}. \tag{14}$$

By integrating Eq. (13), the following is obtained:

$$P(V_1) \propto \exp\left[-\frac{1}{E_{00}}\left((V_B - V)^{1/2}(V_B - V - V_1)^{1/2} - V_1 \times \ln\frac{(V_B - V)^{1/2} + (V_B - V - V_1)^{1/2}}{V_1^{1/2}}\right)\right], \tag{15}$$

where V is the forward-bias voltage.

The thermionic-field-emission current can be expressed as

$$J_{TF} = \int_0^{q(V_B - V)} q v_x(E) N(E) f(E) P[E(V_1)]\,dE, \tag{16}$$

where $N(E)f(E)$ is the electron density in the energy E at the edge ($x = 0$) of the depletion region and the energy $E(V_1)$ of the tunneling probability $P[E(V_1)]$ in Eq. (16) represents qV_1 in Eq. (15).

With respect to the junction transports on amorphous semiconductors, the thermionic-field-emission current [Eq. (16)] cannot be applied directly in the case of amorphous semiconductors since electron collisions within the depletion region cannot be neglected. The tunneling current at $E = qV_1$ can be described as

$$J'(V_1) \propto \int_{qV_1}^{qV_1 + \delta} N'(E) f(E) P[E(V_1)]\,dE, \tag{17}$$

where δ is a parameter much smaller than qV_D, $N'(E)f(E)$

the electron density in the energy E at $x = d_1$, and

$$N'(E) = [4\pi(2m^*)^{3/2}/h^3](E - qV_1)^{1/2}, \quad (18)$$

because the electrons near the bottom (qV_1) of the conduction band at $x = d_1$, are able to tunnel through the barrier from the position d_1 to the metal and the unoccupation probability for electrons in the metal at $E = qV_1$ is nearly unity. The tunneling probability $P(V_1)$ is assumed constant between qV_1 and $qV_1 + \delta$, and the amount of electrons which exist between the bottom (qV_1) of the conduction band and $qV_1 + \delta$ can be assumed to be proportional to $\exp[-(E_F + qV_1)/kT]$. Therefore,

$$J'(V_1) \propto P(V_1) \exp[-(E_F + qV_1)/kT]. \quad (19)$$

The energy qV_{1p} for the peak of the tunneling current is derived as

$$V_{1p} = \frac{V_B - V}{\cosh^2(qE_{00}/kT)}. \quad (20)$$

Assuming that the tunneling current is close to this peak of the tunneling current,

$$J_{DF} \propto \exp(V/E_0), \quad (21)$$

with

$$E_0 = E_{00} \coth(qE_{00}/kT). \quad (22)$$

cosh(qE00/kT)

This diffusion-field-emission current J_{DF} must be a current peculiar to amorphous Schottky barrier junctions. Currents J_F and J_D can be considered as special cases of J_{DF}.

In the special case ($d_1 = 0$) where electrons tunnel through the whole Schottky barrier, this current is the field-emission current and can be derived from Eq. (13) as

$$J_F \propto \exp(V/E_{00}). \quad (23)$$

The slope ($1/E_{00}$) of the $\ln(J)$-V relation does not depend on the temperature, as is clear from Eqs. (14) and (23).

In another special case ($d_1 = d$) where all electrons are diffused over the entire depletion region, this current is called the diffusion current[19] and can be described as

$$J_D \propto qN_C\mu F \exp[-(q\phi_B/kT)]\exp(qV/kT), \quad (24)$$

where F is the electric field in the semiconductor near the metal-semiconductor interface, $q\phi_B$ the barrier height of qV_B plus E_F ($\sim \Delta E_2$), and μ the electron mobility. Since the electric field F varies with the applied voltage, Eq. (24) can be rewritten as

$$J_D \propto \exp(qV/\eta kT), \quad (25)$$

where $\eta = 1.06$.[20,30] The diffusion current J_D is a desirable current in amorphous Schottky barrier junctions.

B. Comparison to experimental results

The current in sample $Y4$ is limited by the field emission described in Eq. (23) and the slope of the J-V characteristics on a semilog scale does not depend on the temperature. The currents in samples $Z2$ and $Z4$ are limited by the diffusion-field emission expressed in Eq. (21) while E_{00} estimated from Eq. (22) using the slope ($1/E_0$) does not depend on the temperature, as shown in Fig. 12. The current in the a-Si:H sample having a good film quality is limited by the diffusion expressed in Eq. (24). Here, the η value (< 1.1) (Ref. 23)

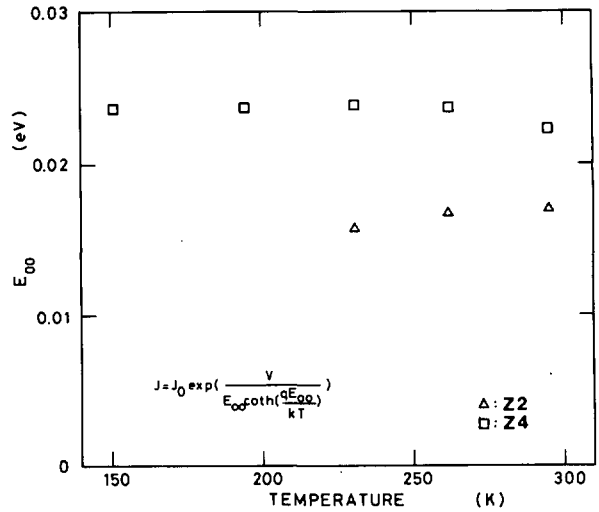

FIG. 12. Temperature dependence of E_{00} estimated from Eq. (22). Those values for samples $Z2$ and $Z4$ are independent of temperatures.

does not depend on the temperature and $q\phi$ estimated from the J-V characteristics is close to the barrier height $q\phi_B$ obtained from the C-V characteristics. The forward-current transports for the Schottky barrier junctions with our a-$Si_{1-x}Ge_x$:H as well as our a-Si:H are roughly grouped as shown in Fig. 13.

The parameters E_{00} which can be calculated from Eq. (14) are 1.76×10^{-3}, 7.18×10^{-4}, and 1.82×10^{-3} eV for samples $Y4$, $Z2$, and $Z4$, respectively, using the N_I obtained from the C-V characteristics, $m^* = m_0 = 9.1\times10^{-31}$ kg, and $\epsilon_s = 16$ obtained from capacitance measurements at the high frequency where the capacitance does not depend on

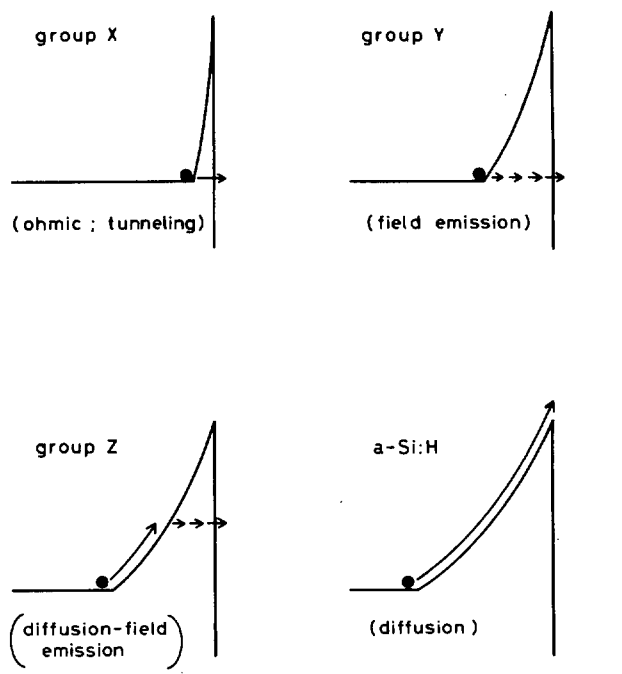

FIG. 13. Four kinds of main forward-current transports. Junctions of groups X, Y, and Z are made of a-$Si_{1-x}Ge_x$:H and deposition conditions of each group are shown in Table I.

the reverse-bias voltage.[12] However, E_{00} obtained graphically from the J-V characteristics are about 3.2×10^{-2} from $E_{00}=1/\beta$ in Fig. 8, 1.7 and 2.3×10^{-2} eV in Fig. 12 for samples $Y4$, $Z2$, and $Z4$, respectively. All of the E_{00} obtained from the J-V characteristics are larger than E_{00} estimated from the C-V characteristics using Eq. (14). This difference results from the multistep tunneling process in amorphous semiconductors, while the one-step tunneling process is assumed in Eq. (14). In the amorphous semiconductors with tail states, E_{00} in Eq. (14) can probably be replaced as

$$E_{00}=[(1+\gamma)h/4\pi]\sqrt{(N_I/m^*\epsilon_0\epsilon_s)}\,, \tag{26}$$

where γ is the multistep tunneling factor and $\gamma=0$ when one-step tunneling process is dominant. Equation (26) probably indicates that electrons can travel a shorter distance than the real distance $(d-d_1)$ as if they can easily move within the localization length or that electrons can flow as if they tunnel through the lower barrier potential than the real barrier potential.[31] More detailed work for understanding of γ is now in progress.

C. General aspects and classification

In our Schottky barrier diodes made of a-$Si_{1-x}Ge_x$:H and a-Si:H films, three kinds of the transport mechanisms of the forward currents were found: (1) the diffusion current in the depletion region, (2) the diffusion-field-emission current, and (3) the field-emission current. The forward current changes J_{DF} into J_F when the effective density N_I of localized states near the Fermi level in the bulk determining the barrier width and/or a density of tail states are considerably high. The diffusion current J_D becomes dominant in place of J_{DF} when the density of localized states which affect the multistep tunneling process is fairly low. It can, moreover, be supposed that the recombination current is dominant in samples with a high density of midgap states mainly affecting the recombination process.

It is difficult to discuss the superiority or inferiority of the amorphous semiconductors in detail from the standpoint of junction properties. Up to now, junction properties are judged only from the rectifying ratio and the diode factor (η value). We, however, could deduce the general aspects of amorphous Schottky barrier junctions from the above discussions; for example, we can discuss superiority or inferiority of the materials in detail using the flow chart shown in Fig. 14.

As the initial step, a metal that forms the Schottky barrier junction with an amorphous semiconductor is searched for among those metals with higher work functions (e.g., Au and Pt) for n-type semiconductors, and metals with lower work functions (e.g., Mg) for p-type semiconductors.[10,13,32–34] When the metal-semiconductor junctions do not exhibit the rectifying properties independent of whether they are formed using metals with higher or lower work function, the amorphous semiconductor used should be classified into grade F.

In the next step, if the forward current does not increase exponentially with the applied voltage although the rectifying property is observed, this material is classified into grade E.

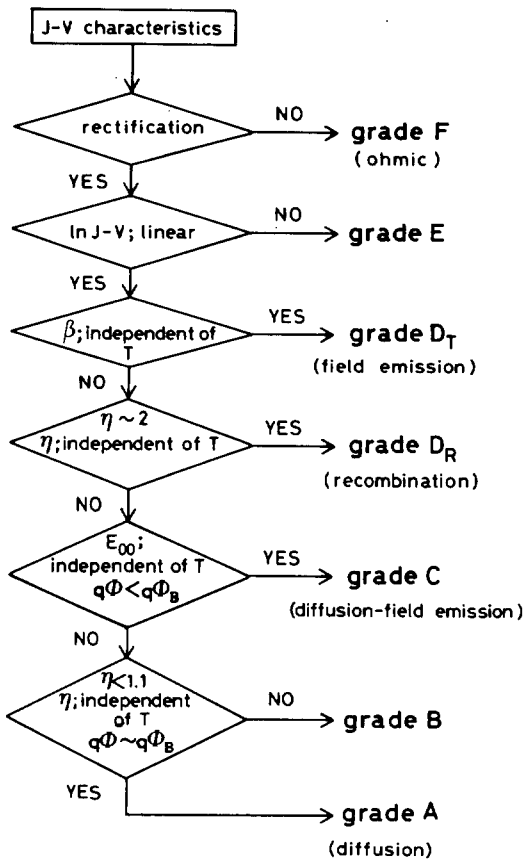

FIG. 14. Flow chart to classify amorphous materials from the standpoint of junction properties. Group X belongs to grades E and F, and group Y is in grades D_T and E. The undoped sample $Z1$ may belong to grade A, while other samples of group Z are of grade C.

The third-step evaluation is based on the temperature dependence of the J-V characteristics. The material with temperature independence for slope β appertains to grade D_T (the field emission). When the η value is close to 2 in the whole range of the measuring temperature, the material belongs to grade D_R (the recombination).

If E_{00} obtained from Eq. (22) does not depend on the temperature and $q\phi<q\phi_B$, the material is classified into grade C (the diffusion-field emission).

When the material does not satisfy at least one of the following conditions: $\eta<1.1$ (Ref. 23), the temperature independence of the η value, and $q\phi\sim q\phi_B$, the diffusion, the recombination, and the diffusion-field-emission currents are mixed into grade B.

Finally, when all of the above conditions are satisfied, this material is most suitable for the junction material and can be classified as grade A (the diffusion).

In the case where the rectifying ratio is not high and/or where the η value is larger than 1.1, one can deduce the more dominant current and can know in detail how the technique of film deposition has been improved from the standpoint of junction properties. For example, we have found that our technique (application of the triode reactor as well as H_2-diluted gas mixtures) is a step in the right direction. We have not, however, achieved the best way as yet and must improve the a-$Si_{1-x}Ge_x$:H materials in the future.

V. CONCLUSION

We have investigated amorphous Schottky barrier junctions using several qualitative $a\text{-Si}_{1-x}\text{Ge}_x\text{:H}$ materials. Although the η values were larger than 1.1, the currents were found to be limited by the multistep tunneling process through the Schottky barrier, and not by the recombination process in the depletion region. A current peculiar to amorphous Schottky barrier junctions is the diffusion-field-emission current proposed in this paper, and is expressed as

$$J \propto \exp(V/E_0),$$

with

$$E_0 = E_{00} \coth^2(qE_{00}/kT)$$

and

$$E_{00} = [(1+\gamma)h/4\pi]\sqrt{(N_I/m^*\epsilon_0\epsilon_s)},$$

where γ is the multistep tunneling factor defined in the text.

When the density of localized states is considerably high, the forward current becomes the field-emission current given by

$$J \propto \exp(V/E_{00}).$$

When it is fairly low, however, the diffusion current becomes dominant, and is described as

$$J \propto \exp(qV/\eta kT),$$

where $\eta < 1.1$.[23]

We could then discuss the general aspects of amorphous Schottky barrier junctions and propose the flow chart shown in Fig. 14 that classifies amorphous semiconductors into six grades. The method (group Z) using the triode reactor as well as H_2-diluted gas mixtures was found to be better for $a\text{-Si}_{1-x}\text{Ge}_x\text{:H}$, as is clear from Figs. 13 and 14.

ACKNOWLEDGMENTS

We wish to thank Dr. A. Matsuda for providing the $a\text{-Si}_{1-x}\text{Ge}_x\text{:H}$ films, and to acknowledge a valuable discussion with Dr. K. Tanaka. We wish to acknowledge our gratitude to the members of the staff of the Amorphous Materials Section in the Electrotechnical Laboratory for their valuable insights and comments. We would also like to thank Y. Imanishi, N. Ikuchi, and H. Kataoka for helping with the sample preparations, and S. Fujita for helping with the measurements.

[1]W. E. Spear and P. G. LeComber, Philos. Mag. **33**, 935 (1976).
[2]D. E. Carlson, in *Semiconductors and Semimetals*, edited by J. I. Pankove (Academic, Orlando, FL, 1984), Vol. 21, part D, p. 7.
[3]P. G. LeComber and W. E. Spear, in *Semiconductors and Semimetals*, edited by J. I. Pankove (Academic, Orlando, FL, 1984), Vol. 21, part D, p. 89.
[4]For a Schottky barrier junction of Si;Ge:H;F: V. Chu, S. Aljishi, D. Slobodin, and S. Wagner, Mater. Res. Soc. Symp. Proc. **70**, 295 (1986).
[5]D. E. Carlson and C. R. Wronski, Appl. Phys. Lett. **28**, 671 (1976).
[6]C. R. Wronski, D. E. Carlson, and R. E. Daniel, Appl. Phys. Lett. **29**, 602 (1976).
[7]A. Deneuville and M. H. Brodsky, J. Appl. Phys. **50**, 1414 (1979).
[8]Y. Mishima, M. Hirose, and Y. Osaka, Jpn. J. Appl. Phys. **20**, 593 (1981).
[9]M. J. Thompson, N. M. Johnson, R. J. Nemanich, and C. C. Tasi, Appl. Phys. Lett. **39**, 274 (1981).
[10]H. Matsuura, T. Okuno, H. Okushi, S. Yamasaki, A. Matsuda, N. Hata, H. Oheda, and K. Tanaka, Jpn. J. Appl. Phys. **22**, L197 (1983).
[11]M. J. Thompson, R. J. Nemanich, and C. C. Tsai, Surf. Sci. **132**, 250 (1983).
[12]H. Matsuura, T. Okuno, H. Okushi, and K. Tanaka, J. Appl. Phys. **55**, 1012 (1984).
[13]H. Matsuura, A. Matsuda, H. Okushi, T. Okuno, and K. Tanaka, Appl. Phys. Lett. **45**, 433 (1984).
[14]R. J. Nemanich, in *Semiconductors and Semimetals*, edited by J. I. Pankove (Academic, Orlando, FL, 1984), Vol. 21, part C, p. 375.
[15]H. Matsuura, A. Matsuda, H. Okushi, and K. Tanaka, J. Appl. Phys. **58**, 1578 (1985).
[16]W. B. Jackson, R. J. Nemanich, M. J. Thompson, and B. Wacker, Phys. Rev. B **33**, 6936 (1986).
[17]A. Matsuda, K. Yagii, M. Koyama, M. Toyama, Y. Imanishi, N. Ikuchi, and K. Tanaka, Appl. Phys. Lett. **47**, 1061 (1985).
[18]A. Matsuda, M. Koyama, N. Ikuchi, Y. Imanishi, and K. Tanaka, Jpn. J. Appl. Phys. **25**, L54 (1986).
[19]S. M. Sze, *Physics of Semiconductor Devices*, 2nd ed. (Wiley-Interscience, New York, 1981), p. 254.
[20]I. Chen and S. Lee, Proceedings of the 9th International Conference on Amorphous and Liquid Semiconductors, Grenoble, 1981; J. Phys. (Paris) **42**, C4-499(1981); J. Appl. Phys. **53**, 1045 (1982).
[21]F. A. Padovani and R. Stratton, Solid State Electron. **9**, 695 (1966).
[22]It is difficult to obtain qV_B by the conventional C-V methods above 1 Hz because of the high resistivity ($\sim 10^9$ Ω cm) in undoped a-Si:H; it was obtained by measuring a difference (a displacement current) in current levels between increasing and decreasing voltage modes of low-frequency (0.01 Hz) triangle-wave excitation, described by H. Okushi, K. Nakagawa, S. Yamasaki, H. Yamamoto, A. Matsuda, M. Matsumura, K. Tanaka, and S. Iizima, Jpn. J. Appl. Phys. **20**, Suppl. 20-2, 205 (1981).
[23]Although the η value should theoretically be 1.06 if the current is dominated by the diffusion, the observed J-V characteristics with η values of less than 1.1 can be attributed to the diffusion current alone, described in Ref. 20.
[24]J. W. Conley, C. B. Duke, G. D. Mahan, and J. J. Tiemann, Phys. Rev. **150**, 466 (1966).
[25]J. W. Conley and G. D. Mahan, Phys. Rev. **161**, 681 (1967).
[26]C. R. Crowell and V. L. Rideout, Solid State Electron. **12**, 89 (1969).
[27]C. R. Crowell and V. L. Rideout, Appl. Phys. Lett. **14**, 85 (1969).
[28]C. Y. Chang and S. M. Sze, Solid State Electron. **13**, 727 (1970).
[29]J. R. Macdonald, Solid State Electron. **5**, 11 (1962).
[30]R. Stratton, Phys. Rev. **126**, 2002 (1962).
[31]A. R. Riben and D. L. Feucht, Int. J. Electron. **20**, 583 (1966).
[32]C. R. Wronski and D. E. Carlson, Solid State Commun. **23**, 421 (1977).
[33]J. Kanicki, M. O. Aboelfotoh, and W. Bauhofer, *Proceedings of the 17th International Conference on Physics of Semiconductors*, edited by J. D. Chadi and W. A. Harrison (Springer, New York, 1985), p. 183.
[34]J. Kanicki and D. Bullock, Mater. Res. Soc. Symp. Proc. **70**, 379 (1986).